Supporting Information

Synergic Thermo- and pH-Sensitive Hybrid Microgels Loaded With Fluorescent Dyes and Ultrasmall Gold Nanoparticles For Photoacoustic Imaging and Photothermal Therapy

Yu Xiao[a], Kartikey Pandey [a], Alba Nicolás-Boluda[b], Delphine Onidas[a], Philippe Nizard[a], Florent Carn[b], Théotim Lucas[b,c], Jérôme Gateau[c], Alberto Martin-Molina[e,f], Manuel Quesada-Pérez[g], Maria del Mar Ramos-Tejada[g], Florence Gazeau*[b], Yun Luo*[a], Claire Mangeney *[a]

a. Université Paris Cité, CNRS Laboratoire de Chimie et de Biochimie Pharmacologiques et Toxicologiques, F-75006 Paris, France
b. Université Paris Cité, CNRS Matière et Systèmes Complexes MSC, F-75006 Paris, France.
c. Sorbonne Université, CNRS, INSERM, Laboratoire d'Imagerie Biomédicale, LIB, F-75006, Paris, France
e. Departamento de Física Aplicada, Universidad de Granada, Campus de Fuentenueva s/n, 18071 Granada, Spain
f. Instituto Carlos I de Física Teórica y Computacional, Universidad de Granada, Campus de Fuentenueva s/n, 18071 Granada, Spain
g. Departamento de Física, Escuela Politécnica Superior de Linares, Universidad de Jaén, 23700, Linares, Jaén, Spain
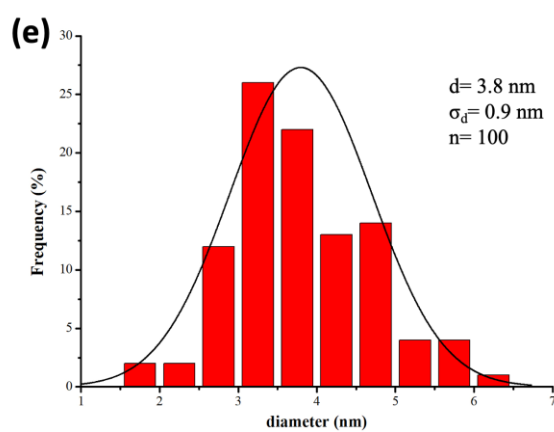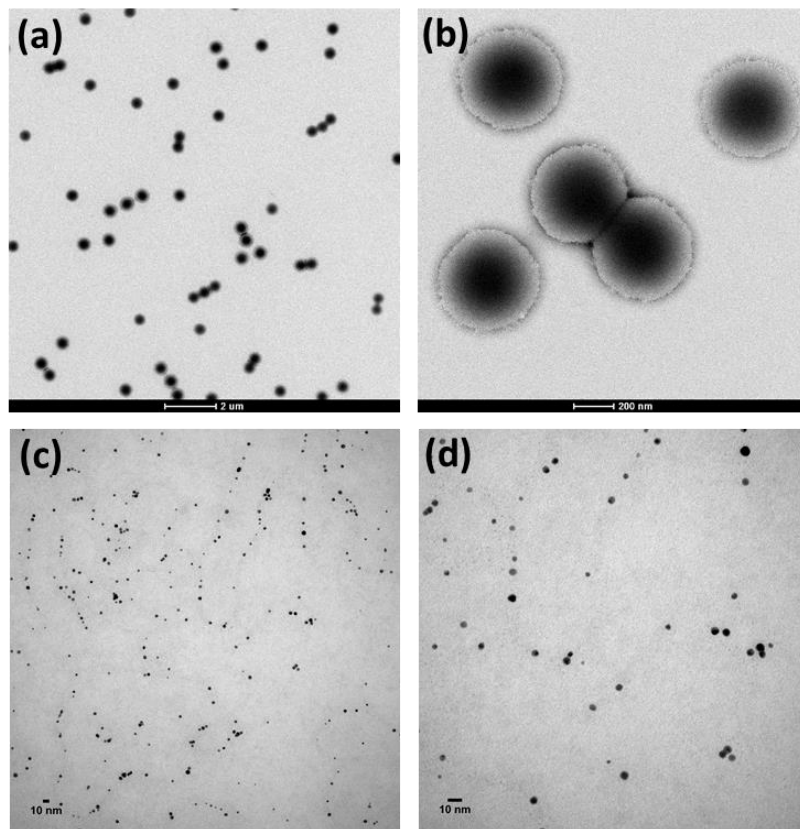
Corresponding Authors

* Claire Mangeney. E-mail : claire.mangeney@u-paris.fr
* Florence Gazeau. Email: florence.gazeau@univ-paris-diderot.fr
* Yun Luo. Email : yun.luo@u-paris.fr

1. CHARACTERIZATION AND SIMULATION OF μGels, Gel@dye AND Gel@dye@Au SAMPLES

● **TEM images of pristine μGels and Au NPs**

Figure S1. TEM images of (a,b) bare μGels and (c,d) Au NPs, at different magnifications. (e) histogram of Au NP diameter measured from TEM. The Au NP size was analyzed on 100 NPs using the software ImageJ.

● **Coarse-grained simulations of the mechanisms driving the assembly process**

Figure S2 displays the number of nanoparticles absorbed per unit of volume (number density) as a function of B_{mn}/k_BT and B_{md}/k_BT for a nanoparticle concentration of $6.022 \cdot 10^{-4}$ nanoparticle/nm^3 (1 mM). In the absence of dyes (black squares and bottom *x*-axis), only B_{mn}/k_BT is considered and the simulation shows that high values of B_{mn}/k_BT (> 30 nm^{-6}) are required to observe a significant increase of the number of absorbed nanoparticles (in spite of the electrostatic repulsive forces between them NPs and nanogel). It is noteworthy that such dispersion constants are not realistic as they are very high compared to the typical values of ions with high polarizability, such as thiocyanate (~ 0.5 nm^{-6}).[1] Therefore, it is most probable that diffusion is the driving mechanism for the absorption of Au NPs in the absence of dyes.
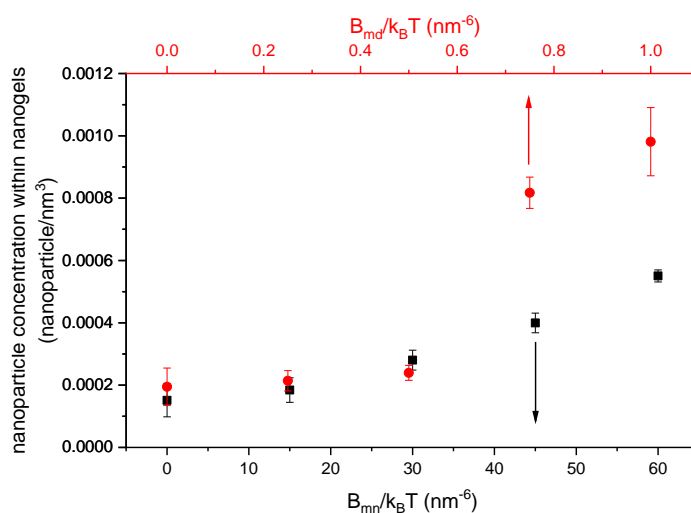
Figure S2. Number density of absorbed nanoparticles as a function of B_{mn}/k_BT (black squares and bottom *x*-axis) and B_{md}/k_BT (red circles and top *x*-axis).

In the presence of the dyes (positively charged species, at $6.022 \cdot 10^{-4}$ molecules/nm^3), the nanoparticle concentration within the nanogel exhibits an abrupt increase for B_{md}/k_BT-values larger than 0.75 nm^{-6} (red circles and top *x*-axis), which can be explained as follows: if the dispersion constant is high enough, the absorption of the dye can be so strong that it causes a reversal of the nanogel charge. In this case, absorption would be also electrostatically driven due to the attractive interactions between the negatively charged NPs and cationic dye-loaded nanogel. It is noteworthy that the concentrations of the various components used in the simulations (nanogel, dyes, nanoparticles) are higher that the experimental ones due to simulation requirements.

● DLS study of Gel@R6G@Au$_{(1)}$, Gel@MB@Au$_{(1)}$ and Gel@Cy@Au$_{(1)}$ as a function of pH and temperature

Study of pH stimulus

Table S1. Hydrodynamic diameters (z-average) of Gel@R6G@Au$_{(1)}$, Gel@MB@Au$_{(1)}$ and Gel@Cy@Au$_{(1)}$ determined by DLS as a function of pH (at 25℃). All Gel@dye@Au$_{(1)}$ samples were prepared from [Dye]$_0$ = 50 μM, after x = 1 incubation cycle with Au NPs solution ([AuNPs] = 0.27 μmol.L^{-1}).

pH	Gel@R6G@Au$_{(1)}$ (nm)	Gel@MB@Au$_{(1)}$ (nm)	Gel@Cy@Au$_{(1)}$ (nm)
2	452.1 ± 2.7	454.6 ± 7.5	480.2 ± 3.3
2.5	452.8 ± 3.7	454.7 ± 10.4	479.8 ± 6.3
3	445.5 ± 12.1	450.5 ± 10.3	479.3 ± 12.3
3.5	462.7 ± 7.5	452.1 ± 9.6	488.6 ± 10.6
4	448.7 ± 9.6	469.9 ± 7.3	482.4 ± 16.0
4.5	447.7 ± 8.4	469.3 ± 12.1	493.0 ± 10.1
5	458.7 ± 6.7	464.9 ± 15.0	517.1 ± 11.9
5.5	449.3 ± 12.8	488.7 ± 1.1	498.1 ± 21.1
6	476.0 ± 4.7	488.8 ± 11.1	526.3 ± 22.5
6.5	459.2 ± 11.1	502 ± 15.1	546.1 ± 15.1
7	488.8 ± 1.76	544.7 ± 14.1	578.7 ± 4.9
7.5	597.4 ± 9.4	605.2 ± 6.5	601.1 ± 3.8
8	633.3 ± 61.9	909.9 ± 82.3	699.5 ± 7.3
8.5	724.9 ± 9.2	1012 ± 9.0	1113.6 ± 70.7
9	1058.6 ± 38.1	994.2 ± 50.6	1023.4 ± 62.8
9.5	1258.0 ± 74.3	1007.2 ± 8.7	1006.8 ± 84.3
10	972.4 ± 15.1	1091 ± 38.3	984.2 ± 103.3

Study of temperature stimulus

Table S2. Hydrodynamic diameters (z-average) of Gel@R6G@Au$_{(1)}$, Gel@MB@Au$_{(1)}$ and Gel@Cy@Au$_{(1)}$ determined by DLS as a function of temperature (at pH 7). All Gel@dye@Au$_{(1)}$ samples were prepared from $[Dye]_0 = 50$ μM, after x = 1 incubation cycle with Au NPs solution ($[AuNPs] = 0.27$ μmol.L^{-1}).

T	Gel@R6G@Au$_{(1)}$ (nm)	Gel@MB@Au$_{(1)}$ (nm)	Gel@Cy@Au$_{(1)}$ (nm)
10	824.4 ± 20.8	687.5 ± 17.9	681.2 ± 6.0
12.5	819.6 ± 21.5	672.4 ± 12.1	676.9 ± 6.8
15	778.9 ± 38.0	672.8 ± 18.3	657.8 ± 7.5
17.5	771.1 ± 34.9	658.4 ± 25.7	644.1 ± 8.9
20	645.4 ± 20.1	604.3 ± 22.4	626.6 ± 1.7
22.5	614.6 ± 25.5	587.9 ± 10.6	617.3 ± 7.4
25	597.4 ± 9.4	565.2 ± 23.4	604.6 ± 7.2
27.5	551.1 ± 14.6	542.0 ± 18.7	578.0 ± 11.8
30	527.5 ± 9.8	524.5 ± 3.9	567.6 ± 3.9
32.5	486.0 ± 13.1	498.6 ± 15.9	525.6 ± 16.1
35	466.0 ± 14.8	474.1 ± 7.8	514.0 ±12.1
37.5	445.3 ± 13.9	439.1 ± 8.7	480.9 ± 2.4
40	441.5 ± 9.5	414.2 ± 1.6	455.1 ± 9.5
42.5	421.8 ± 18.8	396.7 ± 2.6	441.8 ± 4.7
45	407.9 ± 11.4	377.3 ± 11.7	430.3 ± 6.8
47.5	399.4 ± 14.3	369.2 ± 10.0	409.2 ± 7.3
50	397.2 ± 4.7	353.6 ± 7.1	392.7 ± 7.5
52.5	395.9 ± 8.2	359.8 ± 4.1	380.6 ± 7.2
55	398.5 ± 2.8	355.5 ± 10.7	378.3 ± 4.0
57.5	386.7 ± 7.5	353.2 ± 10.9	373.6 ± 4.9
60	391.3 ± 3.9	354.6 ± 8.2	371.9 ± 6.4
62.5	392.3 ± 6.3	353.6 ± 2.0	375.5 ± 2.9
65	397.7 ± 7.5	346.2 ± 13.3	378.6 ± 7.6
65.5	398.6 ± 4.1	344.5 ± 1.2	379.8 ± 4.5
70	393.3 ± 4.4	354.0 ± 6.2	378.2 ± 2.1

Study of the reversibility of the temperature-induced phase transition on Gel@Cy@Au$_{(1)}$ samples
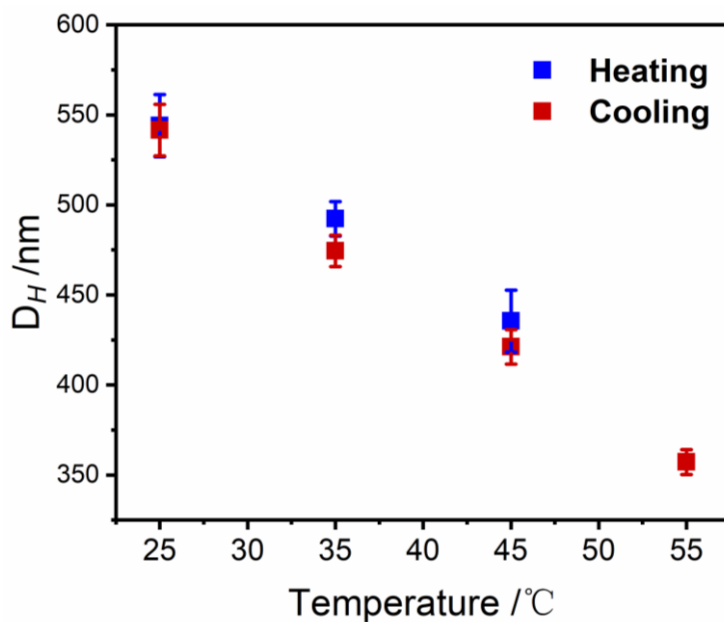
Figure S3. Plots of D$_H$ determined by DLS *vs* temperature (at pH 7) for Gel@Cy@Au$_{(I)}$ hybrid μGels, prepared from [Dye]$_0$ = 50 μM, after x = 1 incubation cycle with Au NPs solution ([AuNPs] = 0.27 μmol.L^{-1}). The blue plot corresponds to the heating cycle followed by the cooling cycle (red plot). It is noteworthy that this reversibility study was performed on a different batch, compared to the one used in Figure 6.

● **SAXS characterization**
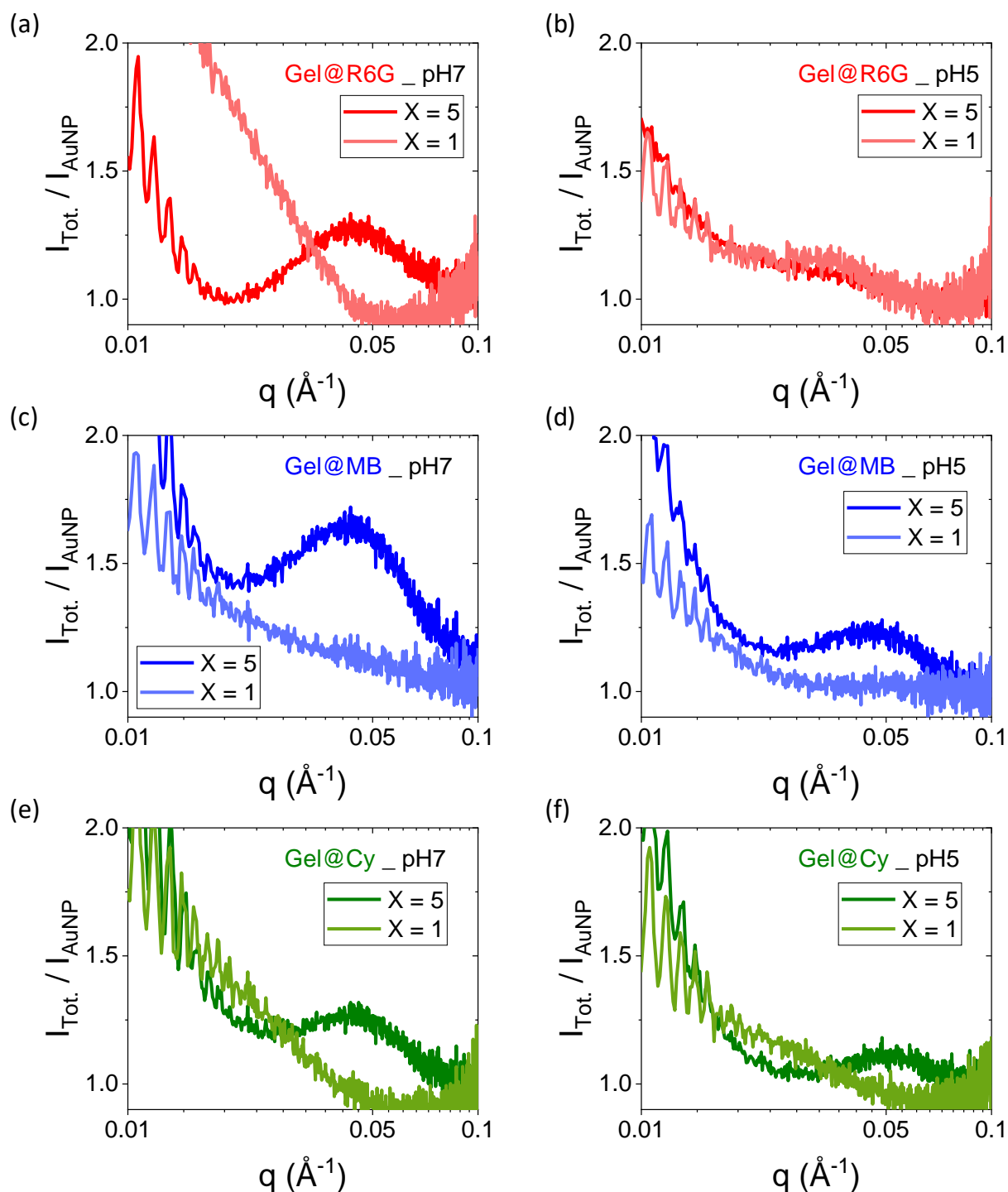
Figure S4. Small angle X-ray scattering (SAXS) characterization of aqueous solutions (pH = 7 or 5) of Gel@dye@Au$_{(x=1, 5)}$, with dye = R6G (a) at pH 7 and (b) at pH 5, MB (c) at pH 7 and (d) at pH 5 and Cy (e) at pH 7 and (f) at pH 5. All measurements were done at room temperature. The curves display the evolution of the ratio between the total intensity ($I_{Tot.}(q)$) scattered by the suspension of Gel@dye@Au$_{(x)}$ and the intensity scattered by a suspension of Au NPs at the same concentration ($I_{AuNP}(q)$) as a function of q.

● **Specific absorption rates (SAR).** The specific absorption rates (SAR) were measured as follows. The initial temperature slopes, dT/dt, after laser switch-on, were measured, and SAR values were calculated according to:

$$SAR = CV/m \times dT/dt \qquad \text{(eq. 1)}$$

where m is the total mass of the materials in the sample (here m = mass of Au NPs for x=1 or x=5, calculated from Table 1: m_{Au}=8.65 µg for x=1 and m_{Au}=43.25 µg for x=5), C is the specific heat capacity of the sample (C_{water} = 4185 J.L^{-1}.K^{-1}), and V is the sample volume (V=100 µL).

● **Cell uptake analysis**
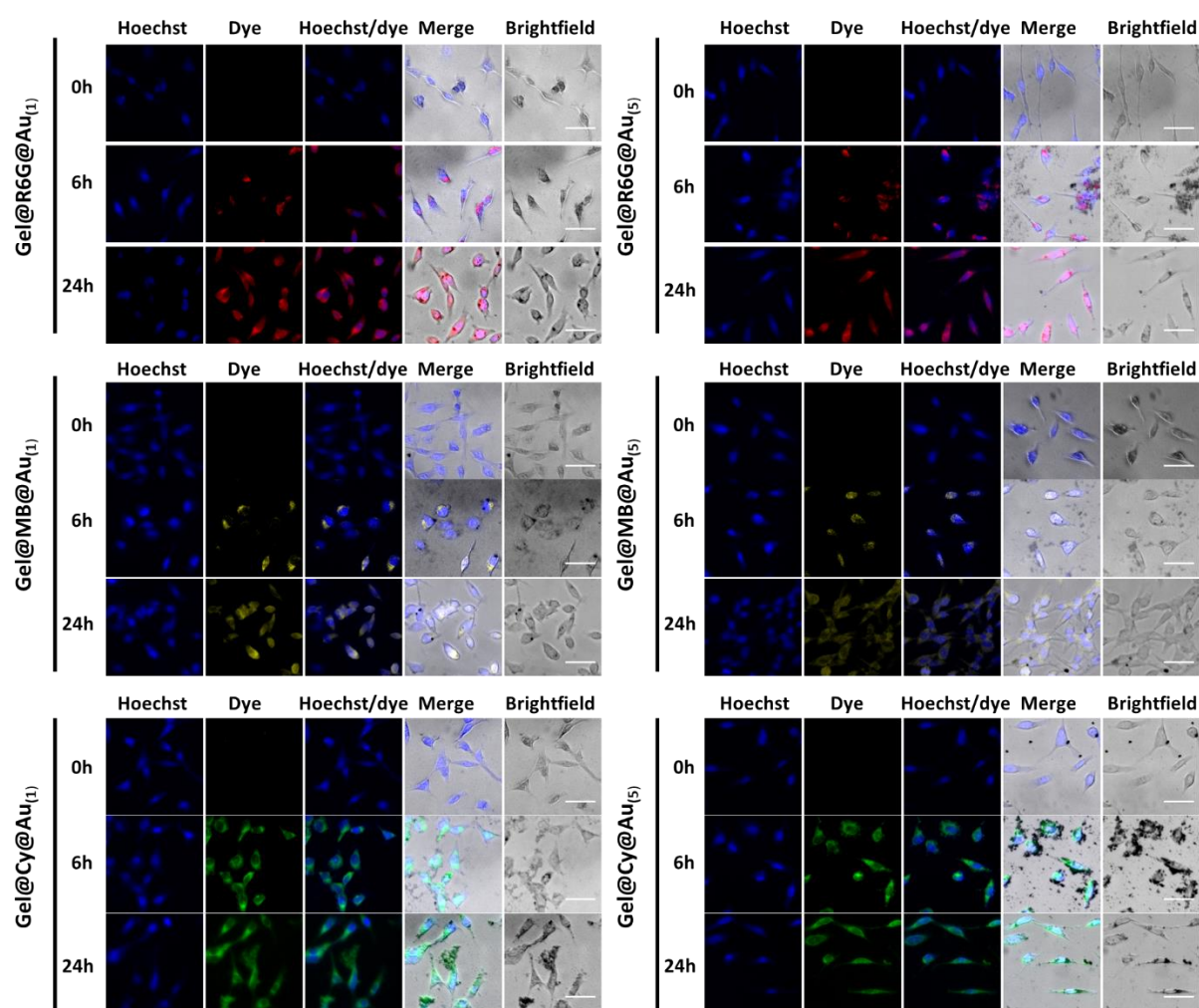
Figure S5. Bright field and fluorescence microscopy of CT26 cells incubated for 24 h with Gel@dye@Au $_{(1\ or\ 5)}$, ([Dye]$_0$ = 250 µM). After washing to remove exceeded µgels, CT26 cells were further incubated for t = 0, 6 h and 24 h and observed by HCS CellInsight CX7. Scale bar = 50 µm.

● **Comparison of normalized PA spectra of Gel@MB, Gel@MB@Au$_{(1)}$, Gel@Cy and Gel@Cy@Au$_{(x=1)}$**

The PA spectra of Gel@MB@Au$_{(1)}$ were measured at pH=7.5 for two concentrations of MB (50 μM and 250 μM). They are displayed in Fig. S6, together with the spectrum of Gel@MB and the spectra of Gel@Cy and Gel@Cy@Au$_{(1)}$ for comparison. Each spectrum was normalized by its maximum for an easier comparison. The absorption above 750 nm becomes significant for Gel@MB@Au$_{(1)}$ while it was negligible for Gel@MB. However, not absorption peak was measured. The peak in the range 750-850 nm for Gel@Cy@Au$_{(1)}$ was therefore associated to the Cy and its broadening and red shift are likely to be linked to coupling between the dye and the Au nanospheres inside the gel.
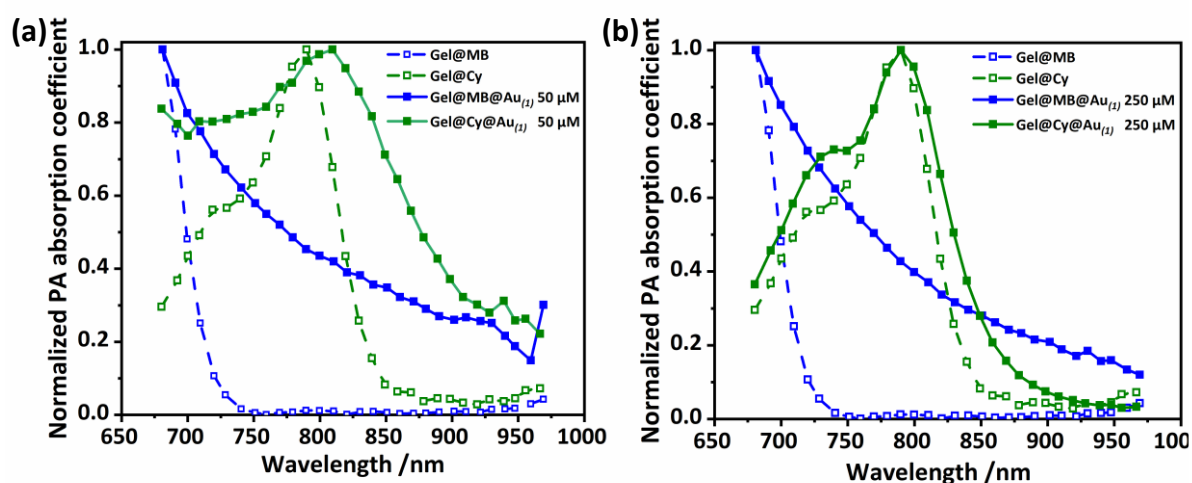
Figure S6. Normalized photoacoustic spectra of Gel@MB and Gel@MB@Au$_{(1)}$ (blue curves) and Gel@Cy and Gel@Cy@Au$_{(x=1)}$ (green curves) at pH 7.5, (a) prepared from [Dye]$_0$ = 50 μM), (b) prepared from [Dye]$_0$ = 250 μM.

1.   Perez-Mas, L.; Martin-Molina, A.; Jain, R. K.; Quesada-Perez, M., Effect of dispersion forces on the behavior of thermosensitive nanogels: A coarse-grained simulation study. *Journal of Molecular Liquids* **2019,** *288*, 111101.